Stanford Exploration Project, Report 94, November 11, 1997, pages 81–90

Stanford Exploration Project, Report 94, November 11, 1997, pages 81–90

3-D prestack datuming in midpoint and offset coordinates

Sean Crawley[1]

keywords: *antialiasing, datuming, upward-continuation, 3-D*

ABSTRACT

3-D seismic surveys are designed to have even sampling in midpoints, but often have irregular sampling in offset. For instance, marine surveys tend towards poor sampling and small aperture in the crossline offset direction, owing to the necessity of towing streamers. Integral operators which work on 3-D prestack data must deal with the problems that arise from 3-D prestack geometry in order to be useful; a straightforward generalization of a 2-D operator is likely to consume a great many CPU cycles to produce suboptimal output. Prestack Kirchhoff datuming can be made more effective in 3-D by reformulating it in midpoint and offset coordinates, and choosing an antialiasing strategy to take advantage of the resulting limitation of the time dip of events.

INTRODUCTION

Irregular spatial sampling complicates integral operators. Nonuniform distribution of fold leads to anomalous amplitudes even for relatively simple models (Chemingui and Biondi, 1996). Variability of spatial sampling can severely complicate antialiasing (Blondel, 1993; Lumley, 1993). One option for dealing with irregularity and uneven sampling is to first regularize the input. AMO (Biondi and Chemingui, 1994) is an example of an operator which regularizes prestack data, by transforming data at assorted offsets and azimuths to a single offset and azimuth. The alternative is to formulate operators which somehow compensate for the irregularity in the input. Here I propose an antialiasing strategy for prestack datuming which attempts to compensate for the poor crossline sampling and aperture of a prestack 3-D marine survey.

An operator is antialiased when crossing plane waves (hyperbola flanks) are orthogonal (Claerbout, 1995). Generally speaking, if the data are poorly sampled and contain many dips, the situation is hopeless, because the operator will either bandpass dipping events into oblivion or alias them. If some limiting assumption can be made

[1]**email:** sean@sep.stanford.edu

about the dips present in the data, then whatever operator bandwidth is available can be centered around those dips, and more frequency preserved in the output.

In my proposed operator, datuming is performed in midpoint and offset coordinates. This has the considerable benefit that energy moves across crossline midpoints with high bandwidth, even when sampling is poor. Datuming in midpoint and offset coordinates still has the appearance of spraying hyperbolas with smoothed flanks. However, consideration of the traveltime paths (shown in Figure 1) shows that the largest bandwidth plane waves dip to propagate along midpoint dip, while the source and receiver datuming operator always has its maximum bandwidth traveling vertical. Projecting the traveltime paths into the subsurface suggests that many structural dips can be better upward continued by the midpoint and offset version of the operator.

Also, in midpoint and offset coordinates there are assumptions that can potentially be made about the time dips in the data, to further increase operator bandwidth. A principal time dip for antialiasing is chosen to correspond to source and receiver rays which converge at some depth. In the limiting case (also the easiest case and the one used here), the depth is infinite, the rays are parallel, and in common midpoint gathers the operator has maximum bandwidth predictably at its top. That can easily be tuned to some finite depth to favor a particular dataset; it could even be depth-variable. Depth-variable principle time dip would require a more costly time-domain operator, because the time dip used to compute the width of smoothing would be time-dependent, but might pay off with spectacular bandwidth.

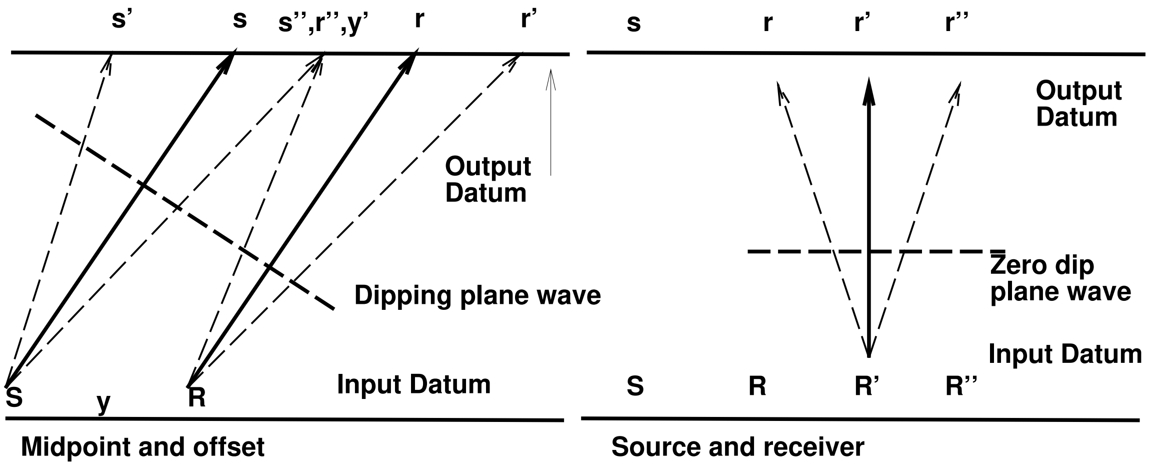

Figure 1: Datuming in midpoints and offsets antialiases with respect to dipping plane waves for nonzero midpoint dip. Datuming in source and receiver coordinates considers vertically propagating plane waves. sean1-pic0 [NR]

PRESTACK DATUMING

Midpoint and offset

Datuming is generally formulated in separate steps for source gathers and receiver gathers, because this is most efficient. In 3-D, the large variability between inline and crossline sampling makes this a less obvious choice. Sticking to marine geometry, datuming receiver and source gathers separately inhibits energy from moving with high bandwidth in the crossline direction. Moving the operator to midpoint and offset coordinates makes it more expensive, because the operator does not separate along midpoint and offset axes the way it does along shot and receiver axes. However, in the case of poorly sampled data it can help by allowing energy to move along the crossline midpoint axis with greater bandwidth.

For each source-receiver pair at the output datum, the greatest bandwidth is given to the input trace whose source-to-source and receiver-to-receiver traveltime paths converge at some chosen depth in the subsurface. Here I choose the depth to be infinite, as shown in Figure 2. For input midpoint y and output midpoint y', the operator has maximum bandwidth where it follows the solid rays from S to s and R to r. The bandwidth decreases as the angle $\theta = \alpha_s + \alpha_r$ increases. This is not a good choice for respecting shallow reflectors and/or long offsets; paths from the input source/receiver pair S and R to output pair s' and r' may be a better choice, because (depending on velocity) they converge at finite depth in the subsurface. The third pair, S to s'' and R to r'', only converge in the subsurface if velocity is sufficiently complex that rays are overturned.

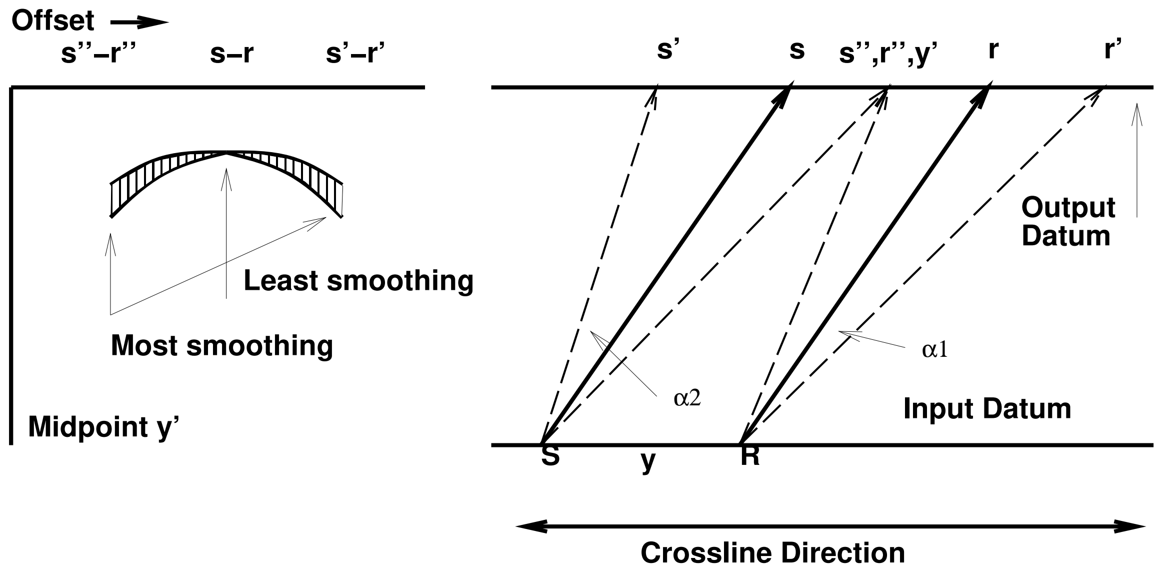

Figure 2: Datuming in midpoint and offset allows poorly sampled energy to cross midpoints with high bandwidth. sean1-pic [NR]

The parallel (infinite reflector depth) traveltime paths give the shortest lag between input and output datum. This means that the least smoothing occurs at the top of the hyperbola in the output. Choosing the increasing offset traveltime paths (S to s', R to r'), or the paths which will generally converge in the subsurface, means the least smoothing occurs at a point on the hyperbola dipping towards increasing offset, which is also generally how seismic events are expected to dip (see Figure 3). Choosing the decreasing offset traveltime paths (S to s'', R to r''), means the rays only converge in the subsurface if velocity is very complex. It also means that the least smoothing on the hyperbola is where it dips to decreasing offset (and seismic events only dip towards decreasing offset in CMP gathers in the case of complex velocity).

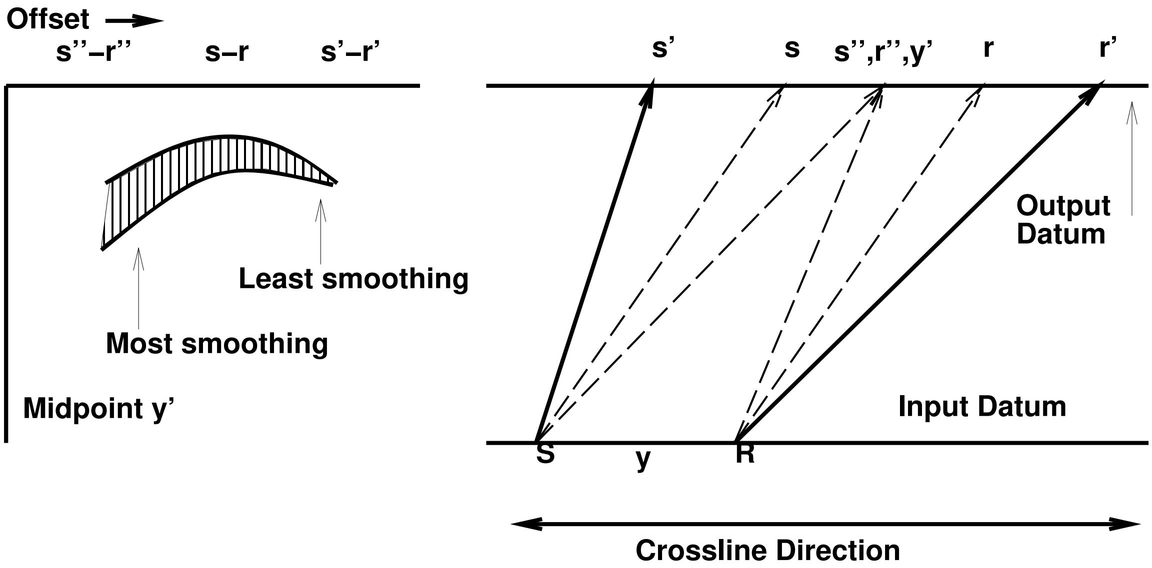

Figure 3: Selecting time dip for traveltime paths which converge in the subsurface gives maximum bandwidth to the part of the operator which dips to increasing offset. sean1-pic2 [NR]

Because the operator is more efficient in frequency and space than in time, I determine a threshold frequency rather than convolve with triangles. To be unaliased, a dipping plane wave must reach adjacent surface points within a half wavelength, which yields the well-known relation

$$f_{th} = \frac{v}{4 \Delta x \sin \theta}$$

where f_{th} is the highest unaliased frequency, v is velocity, Δx is spatial sampling interval, and θ is the plane wave's angle of propagation with respect to vertical, or with respect to a vertically traveling plane wave. For the case of infinite depth reflectors, I substitute the angle between the upward continuation traveltime paths for θ. This is antialiasing the operator with respect to a plane wave with dip equal to the dip between the input and output midpoint.

Future work

One of the issues which I am dealing with in a simplified manner in this paper is output spacing. Lumley (1993) uses the rms of source and receiver inline and crossline spacings. The field data test in this paper is marine, and the synthetics are quasi-marine in their acquisition geometry. For marine geometry it is easy to classify inline aliasing as a second order concern relative to crossline, and essentially ignore it except in the case that energy moves strictly inline. However, the next step in this project is to antialias more difficult land geometries, in particular orthogonal geometries where sources are sparse inline and dense crossline; this will require some more sophisticated answer to the question of spatial sampling.

Also simplified in this project so far is the issue of amplitudes. The amplitude term given by Kirchhoff theory is

$$\frac{\Delta x \Delta y}{2\pi r_{ij} v} \cos\theta_{ij}$$

where r_{ij} connects input point i and output point j, and θ_{ij} is the angle between the normal to the input surface and the traveltime path. This assumes constant sampling and velocity, and infinite aperture, which are in many cases not even approximately realized. In many examples I have found that simpler weights such as $\cos\theta/rv$ or even just unity yield preferable outputs. Intelligent weighting is a future project.

Cost and Alternatives

Datuming as proposed is very expensive because you must do calculations for every couple of source-receiver pairs, within a reasonable aperture, because the operator does not separate. Instead of wave equation upward continuation, Schneider (1995) uses a dynamic time shift for efficient 3-D water layer replacement. The dynamic shifting approach has the benefit that it is very fast, but also the drawback that it is really a 1-D operator. Prestack datuming in midpoint in offset coordinates is quite expensive, but can be made less so by selectively limiting the range of offsets and azimuths from each input midpoint which contribute to a given output trace. In the limiting case the datuming operator bears some resemblance to the common azimuth migration operator of Biondi (1994).

TESTS

Synthetic Data

I tested the method on two synthetics, a simple layer model and a point diffractor model. The synthetic reflector example is boring, but illustrates the point that the integral operator can be safely antialiased in poorly sampled data, allow high frequency energy moving crossline, and maintain high bandwidth in the output. The layer synthetic after upward continuation is shown in Figure 4. The left side of the figure shows the data after upward continuation without any antialiasing. The right side shows the data after upward continuation with antialiasing. The reflection appears to have been 'safely' antialiased but still has excellent frequency content.

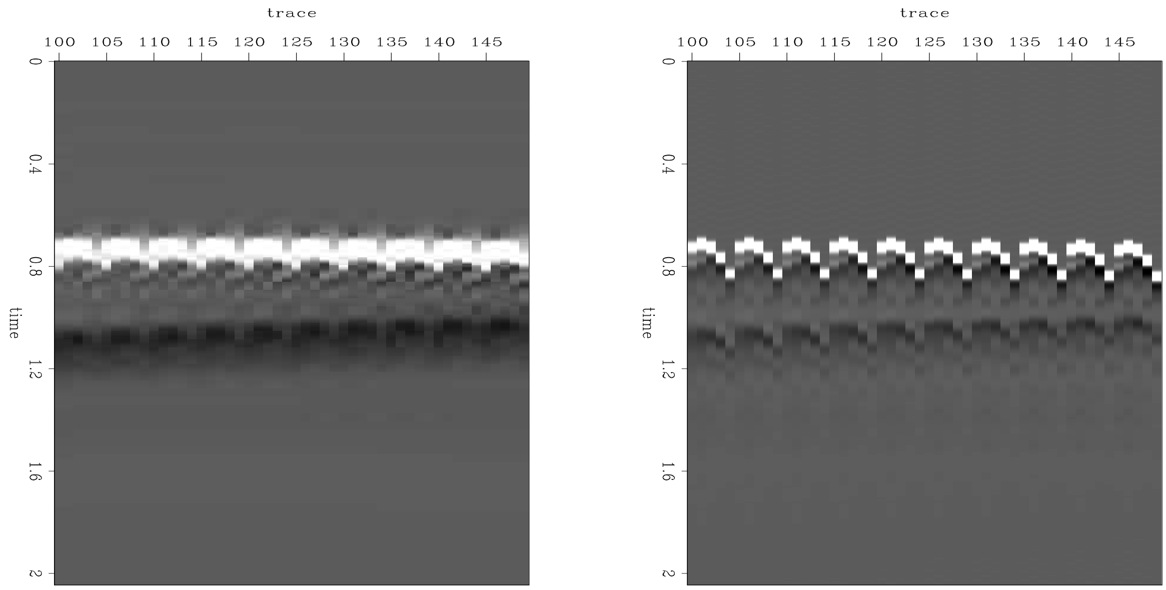

Figure 4: Crosslines from upward continued layer synthetic without (left) and with (right) antialiasing. Antialiasing results in more bandwidth in the output. The input is not shown. The dark artifact .4 s below the reflection is present in the input; it is caused by the Kirchhoff modeling routine. sean1-layer [CR]

The point diffractor example, shown in Figure 5, is more difficult, because the geologic structures exist at individual midpoints. The example is also a difficult test because it has some barely distinguishable events, and because upward continuation will flatten moveouts, the overlapping events at 1.6 s in the input (shown on the left) are bound to be pushed together even more. Though the output (right) shows some degradation and low pass, it is good to see that the overlapping events are still somewhat distinguishable.

Field Data

I also tested the method on a portion of a real 3-D marine data set. The test is very small, because I have not yet done the necessary software engineering to make the code work quickly on a large data set. A portion of the input data is shown in Figure 6, and the corresponding part of the output Figure 7. The output have been rotated in time to make comparison with the input easier.

What is encouraging about the results is that most of the reflectors are easily visible in the output, have not been damaged by aliasing, and in some cases are more

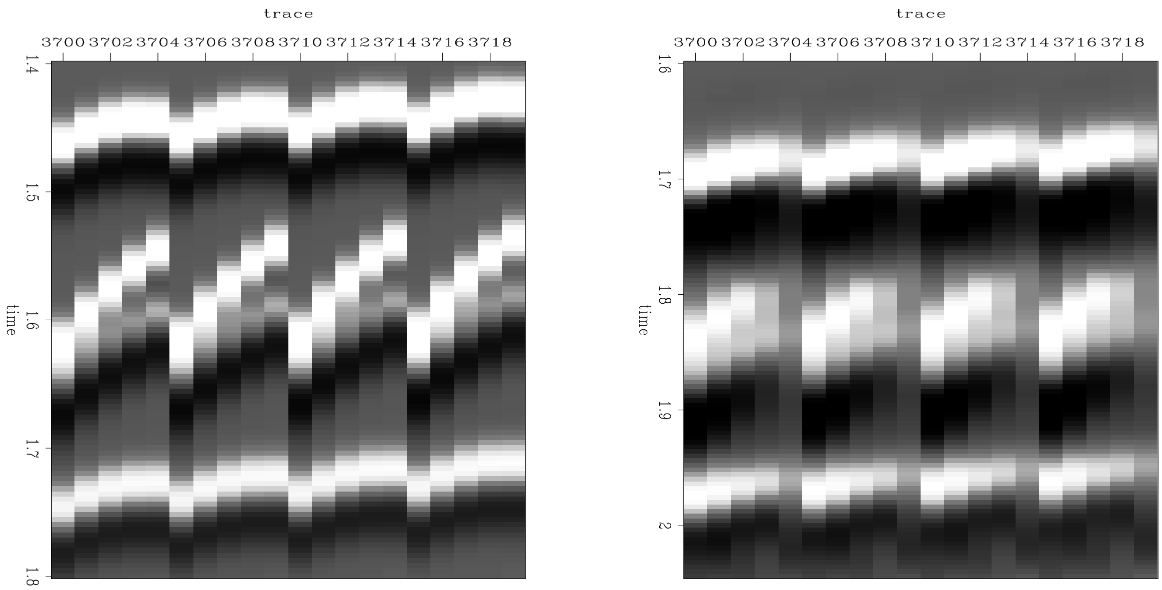

Figure 5: Crosslines from synthetic point scatter data (left), and after upward continuation (right). This is a difficult test because nearly identical input moveouts are flattened and pushed together more by upward continuation. sean1-pointScat [CR]

coherent than in the input (in particular the reflector at approx. 1.55 s). What is discouraging is that certain reflectors, especially those in the neighborhood of 1.3 s, which are somewhat less consistent from input gather to input gather, have been strongly attenuated in the output. I am hopeful that it will turn out this is an artifact of the input data set's size and the necessarily small aperture. I am encouraged that events such as the one at 1.25 s die out as they approach zero inline offset. Also discouraging is the glaring artifact at 1.3 to 1.4 s, in the steep moveout traces. For the most part this artifact is in the mute zone of the traces where it appears, but that isn't true everywhere. It looks disturbingly like a replication of the event at 1.8 s. The code is not well tested, I suspect some technical problem.

CONCLUSION

There is much room for improvement in the method. The incarnation of the antialiasing method presented here is first pass, taking advantage of simplifying factors in marine geometry. Luckily, the acquisition parameters which make orthogonal 3-D land geometries more challenging to program also make the data better suited, in a sense, to upward continuation (larger crossline aperture, finer crossline source sampling).

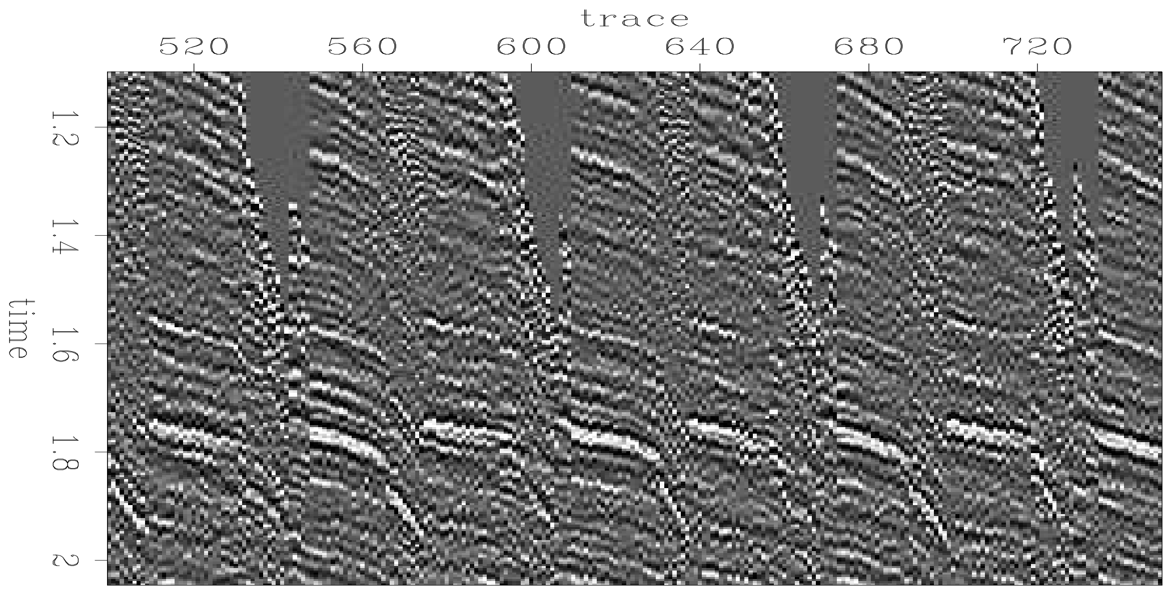

Figure 6: Inlines from input 3-D marine data. sean1-fieldIn [CR]

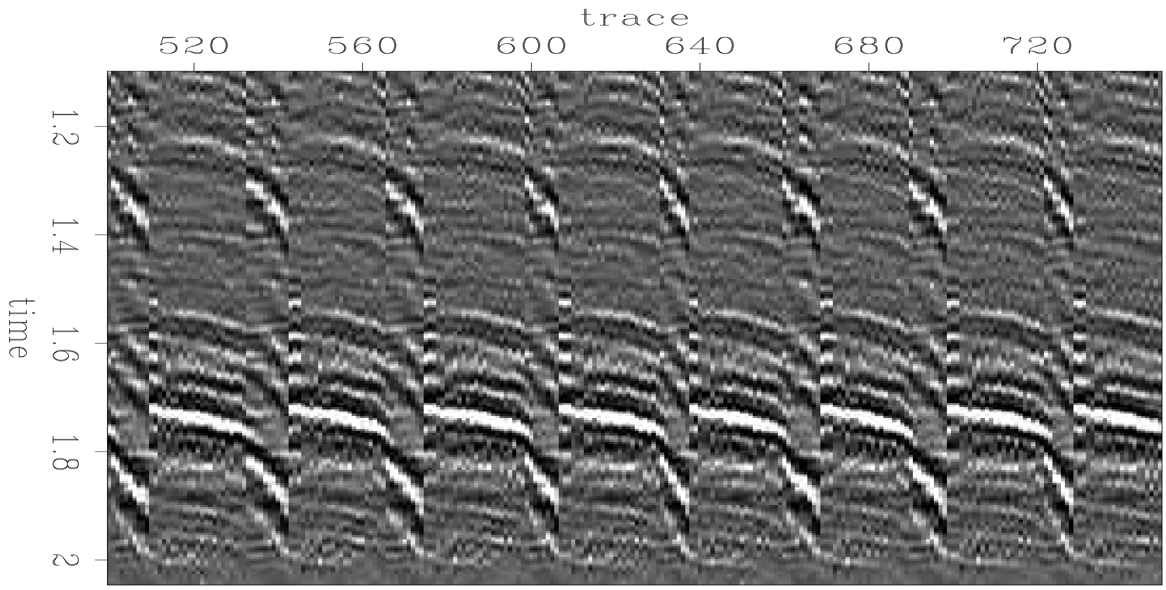

Figure 7: 3-D marine data after upward continuation. sean1-fieldOut [CR]

REFERENCES

Biondi, B., and Chemingui, N., 1994, Transformation of 3-D prestack data by Azimuth Moveout: SEP–**80**, 125–143.

Biondi, B., and Palacharla, G., 1994, 3-D prestack migration of common-azimuth data: SEP–**80**, 109–124.

Blondel, P., 1993, Constant-velocity anti-aliasing three-dimensional integral dip moveout: SEP–**77**, 49–58.

Chemingui, N., and Biondi, B., 1996, Handling irregular geometry in wide azimuth surveys: SEP–**92**, 13–28.

Claerbout, J. F., 1995, Basic Earth Imaging: Stanford Exploration Project.

Lumley, D. E., 1993, Anti-aliased Kirchhoff 3-D migration: A salt intrusion example: SEP–**77**, 1–18.

Schneider, W. A., 1995, Curved-ray replacement dynamics for 3-D marine data: 65th Annual Internat. Mtg., Soc. Expl. Geophys., Expanded Abstracts, 1417–1420.